ISSN 0018-1439, High Energy Chemistry, 2016, Vol. 50, No. 4, pp. 292–297. © Pleiades Publishing, Ltd., 2016.
Original Russian Text © E.B. Gordon, A.V. Karabulin, V.I. Matyushenko, V.D. Sizov, T.N. Rostovshchikova, S.A. Nikolaev, E.S. Lokteva, E.V. Golubina, K.I. Maslakov, I.N. Krotova, S.A. Gurevich, V.M. Kozhevin, D.A. Yavsin, 2016, published in Khimiya Vysokikh Energii, 2016, Vol. 50, No. 4, pp. 305–310.

CHEMISTRY OF NANOSIZED SYSTEMS

Catalysis of Carbon Monoxide Oxidation with Oxygen in the Presence of Palladium Nanowires and Nanoparticles

E. B. Gordon[a], A. V. Karabulin[b], V. I. Matyushenko[c], V. D. Sizov[c], T. N. Rostovshchikova[d], S. A. Nikolaev[d], E. S. Lokteva[d], E. V. Golubina[d], K. I. Maslakov[d], I. N. Krotova[d], S. A. Gurevich[e], V. M. Kozhevin[e], and D. A. Yavsin[e]

[a] *Institute of Problems of Chemical Physics, Russian Academy of Sciences, Chernogolovka, Moscow oblast, Russia*
[b] *MEPhI National Nuclear Research University, Moscow, Russia*
[c] *Talrose Institute of Energy Problems of Chemical Physics, Chernogolovka Branch, Russian Academy of Sciences, Chernogolovka, Moscow oblast, Russia*
[d] *Moscow State University, Moscow, Russia*
[e] *Ioffe Physicotechnical Institute, Russian Academy of Sciences, Moscow, Russia*
e-mail: gordon@ficp.ac.ru

Received November 11, 2015; in final form, December 29, 2015

Abstract—A new synthesis method based on the coagulation of metal nanoparticles, introduced by laser ablation into superfluid helium, inside of quantized vortices has been used for the fabrication of nanoweb consisting of interconnected palladium wires of a 4 nm diameter. It has been found that at temperatures above 523 K, the Pd nanoweb effectively catalyzes the oxidation of CO with molecular oxygen. Temperature cycling leads to a shift of Pd nanoweb activity to lower temperatures. The catalytic action of the Pd nanoweb has been compared to that of Pd nanoparticles with a diameter of about 2 nm prepared by laser electrodispersion.

DOI: 10.1134/S0018143916040068

Carbon monoxide oxidation is widely used as a test process for solving fundamental problems of heterogeneous catalysis [1, 2]. This reaction is an effective tool for studying the dependence of catalytic activity on the size, morphology, charge state, and other structural features of metal nanostructures [3–5]. The regularities of CO oxidation in the presence of a variety of catalysts, such as gas-suspended metal clusters, deposited nanoparticles, single-crystal faces, metal and oxide thin films; have been studied including the process at elevated pressures and temperatures [1–7]. An analysis of published data shows that the role of the assembling of nanoparticles and the nature of the carrier on which they are supported in catalytic activity remains an open question. To clarify the issue, it is desirable to use catalysts having fixed characteristics, such as size, shape, and relative arrangement of nanoparticles.

An important factor that determines the activity of nanocatalysts is the surface curvature of nanostructures [1–7], so small nanowires (NWs) and nanoparticles (NPs) that are close in diameter should have comparably high activity. For example, it was recently found that thin PtFe–FeO_x nanowires supported on TiO_2 catalyze the CO oxidation reaction with oxygen even at 298 K [8]. High activity of the PtFe–FeO_x nanowires was supposed to be due to the presence of interfaces on which the reactants are activated. It is worth noting that Zhu et al. [8] had to use TiO_2 as a support to immobilize short PtFe–FeO_x NWs. As a result, the contribution of the support to the overall activity of the Pt–Fe catalyst was not elucidated.

The use of the technique of laser ablation into superfluid helium for the synthesis of webs of interconnected nanowires makes it possible to eliminate the interaction between the active phase of the catalyst and the support proper [9–11]. As a result, the treatment of the "structure–property" relations for the catalyst becomes unequivocal. In [12] we revealed the specifics of catalysis by a nanoweb composed of copper-alloyed gold nanowires. However, it turned out that NWs of less than 5 nm in diameter had low thermal stability and degraded at temperatures substantially lower than the melting point of the metal from which they had been made [13]. As a result, the nanowires that we synthesized from gold and copper fell apart during the heating of the reactor to the onset temperature of CO oxidation and, therefore, the catalyst was represented by NW fragments and single NPs [12].

Thus, it seemed promising to use as a catalyst nanowebs made of more refractory metals. An important advantage of our research group is the possibility of growing nanowebs of any metal and alloy in quantities sufficient for use as a catalyst for flow catalytic units. The physical principle of our method [9–13] is the possibility of concentrating any nanoparticles, introduced into superfluid helium, in the core of quasi-quantized vortices resulting from almost any

fluid perturbation [14]. Therefore, nanowires can be grown from any metal or alloy. Another advantage of the method is the purity of the metal surface: nanowires are free from the influence of the remnants of precursors and stabilizers adsorbed on the surface of the nanostructures fabricated using the "wet" chemistry techniques [3, 8, 15, 16].

To obtain a catalyst having a nanoweb structure at temperatures high enough for occurrence of a catalytic reaction, we investigated nanowires made from palladium, which is active in CO oxidation [1–5] and is more refractory than gold used in [12]. The melting points of Pd and Au are 1827 and 1337 K, respectively. The nanoweb of palladium NWs was used to catalyze the CO oxidation reaction with molecular oxygen at 273–723 K. For correct analysis, the activities of Pd nanowires synthesized in superfluid helium and Pd nanoparticles prepared by laser electrodispersion (LED) were compared under similar conditions [17–20].

EXPERIMENTAL

Synthesis of Nanowires

Palladium nanowires were obtained on a pilot unit (Institute of Problems of Chemical Physics) assembled on the basis of an optical helium cryostat [9–14]. Palladium atoms and small clusters were injected in superfluid helium at 1.7 K by laser ablation from the surface of a reagent-grade (99.97%) palladium plate immersed in liquid helium. For ablation, an STA-01 diode-pumped Nd:LSB solid-state micro laser available from Standa was used. The main characteristics of the laser were as follows: wavelength, 1.06 μm; pulse repetition rate, 1–4 kHz; pulse energy, ~100 μJ; and pulse width, 0.4 ns. The laser beam was focused by a lens on the target in a spot of about 100 μm in diameter; the average energy density per pulse was about 1 J/cm^2. During irradiation, a pit was formed on the target surface and the incident energy density dropped by increasing the irradiated surface; hence, the amount of metal evaporated per pulse decreased. Therefore, the focal spot was moved over the target, which is a usual thing with laser ablation. Since there was no dependence of the results of coagulation on the pulse repetition rate, the maximum frequency of 4 kHz was generally used. Due to a relatively short radiation pulse, the STA-01 laser allowed effective ablation at a low energy per pulse even for metals with a high thermal conductivity.

In the NW synthesis in superfluid helium, the template to ensure the growth of the condensation product only in one direction is quasi-one-dimensional quantized vortices entraining in their core palladium introduced into superfluid helium. The final condensation product is a nanoweb consisting of nanowires, interconnected by metal bonding, of equal (but characteristic for each metal) thickness. The average length of each wire making the nanoweb was about 200 nm in our experiments. The nanowires formed in the bulk of superfluid helium drew to the bottom of the reactor under the influence of gravity.

To determine the morphology of the nanowires, standard carbon-coated copper grids with a hole diameter of 2 to 3 μm, used transmission electron microscopy (TEM), were placed on the bottom of the reactor. After warming the cryostat to room temperature, the grids were transferred to an electron microscope. Note that prior to TEM examination, the grids were in contact with ambient air for a rather long time.

To obtain nanowires in an amount sufficient for testing the catalytic activity, the laser ablation time was increased to 20 min. In this case, a microporous glass filter of 1.4 cm in diameter and 0.1 cm in thickness was placed at the bottom of the reactor. The nanoweb was deposited on the filter, covering it with a layer of 20–30 nm. During this time, about 10^{18} atoms or a little more than 1 mol of Pd settled on the filter. The filter with Pd nanowires was subsequently used as a catalyst placed in the reactant stream.

Synthesis of Nanoparticles

For a comparative analysis, palladium nanoparticles were used as a catalyst. The LED technique used for their synthesis [17–19] is also based on the ablation of a metal target by a pulse-periodic laser, although in a gas in which the primary products—microdroplets of molten metal—are broken up to nanoparticles and then deposited on the support surface by an electric field. To determine the morphology of the nanoparticles, they were also deposited on TEM grids. For catalytic experiments, the NPs were deposited onto the surface of γ-Al_2O_3 (180 m^2/g, AOK-63-11V, Angarsk catalysts and organic synthesis plant, grain size of 0.4–1 mm) using the LED procedure described in [17–19]. A thin layer of γ-Al_2O_3 grains was placed in a special cell on the surface of a piezoceramic holder. The uniformity of coating the support surface with metal nanoparticles was ensured by shaking the piezoceramic plate. The Pd content of the Pd/Al_2O_3 sample according to atomic absorption spectroscopy data (Thermo iCE 3000 AAS) was 0.005 wt %, an amount that is comparable with the metal content in the glass filter-supported nanoweb.

Analysis of Catalyst Structure

Photomicrographs of nanowires and nanoparticles were obtained using transmission electron microscopy with a Jeol JEM 2100F/UHR instrument at a resolution of 0.1 nm as described in [21, 22]. X-ray photoelectron spectroscopy (XPS) was used to obtain Pd(3*d*) spectra of NWs and NPs on a Kratos Axis Ultra DLD instrument (AlK_α radiation, 1486.6 eV) according to a procedure described in [19]. The XPS spectra

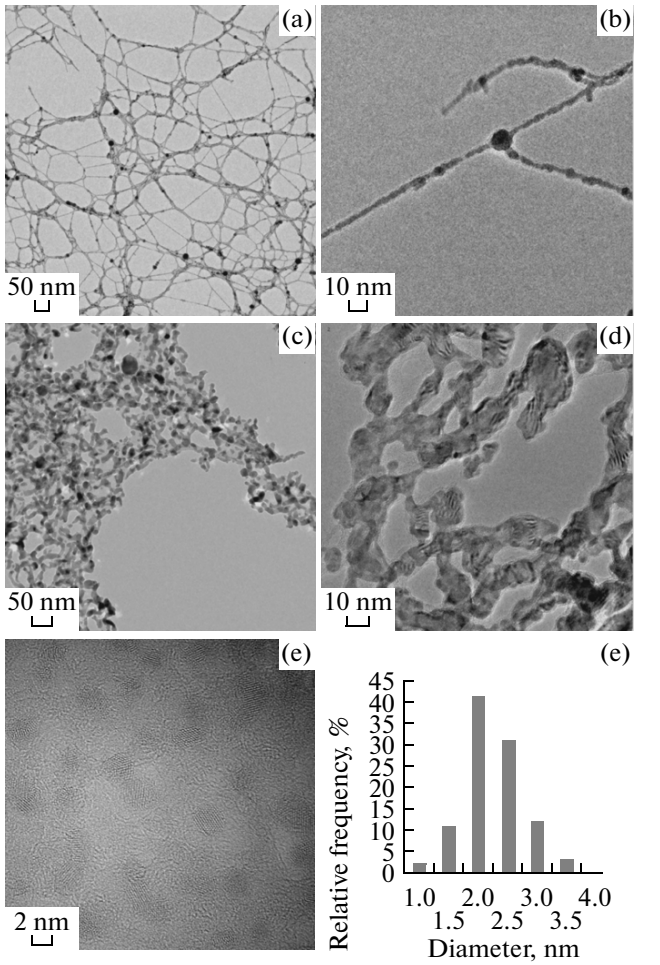

Fig. 1. Micrographs of (a, b) initial nanowires, (c, d) the nanowires calcined at 623 K, and (e) initial nanoparticles. (f) Histogram of size distribution of the initial nanoparticles.

were recorded using an analyzer pass energy of 10–40 eV with a step size of 0.02–0.05 eV. A preliminarily made calibration of the energy scale corresponded to the external standard peak of Au ($4f_{7/2}$) at 83.96 eV.

Oxidation of Carbon Monoxide

The CO oxidation reaction was conducted in the pulse microcatalytic mode in a quartz reactor at atmospheric pressure in the temperature range of 298–723 K [12, 19, 23]. In a typical experiment, two stacked NW-supporting filters or 0.2 g of NP-supporting Al_2O_3 granules was placed in the reactor. The reactor was heated to the desired temperature and the 2% CO + 1% O_2 + 97% He mixture was injected in the reactor in portions of $V = 1$ mL. The composition of the mixture leaving the reactor was determined by gas chromatography on an LKhM-8MD instrument (packed column, $l = 1$ m; phase, Porapak Q; carrier gas He; thermal conductivity detector). The CO conversion was calculated as $\alpha = S(CO_2) \cdot [S(CO_2) + S(CO)]^{-1}$, where S is the area of the respective chromatographic peak. The temperature dependence curve of CO conversion was constructed using a steady-state value of the CO conversion measured after 10–30 injections.

RESULTS AND DISCUSSION

Morphology and Chemical Composition of Nanowires and Nanoparticles

Figures 1a and 1b present photomicrographs of the nanowires prepared by laser ablation into superfluid helium. It is evident that the NWs have a diameter of 4 nm and form a coherent structure hanging as a whole in the TEM grid holes. Assuming that NWs are the main condensation product, we can estimate their full length at about 2×10^6 m and the total surface area at about 0.02 m^2. To analyze thermal stability of the nanoweb, the grid with NWs was heated in air to 623 K and held at this temperature for 1 h. As can be seen from Figs. 1c and 1d, heating to a temperature of about three times below the Pd melting point already leads to the disintegration of the nanowires into chains with units of a 10–40 nm length and a 4–5 nm diameter. Figures 1d and 1e shows TEM images of nanoparticles prepared by the LED technique. It is seen that the NPs are evenly distributed over the surface of the TEM grid and have a spherical shape with an average diameter of about 2 nm.

The XPS spectra of NWs and NPs contain a doublet of Pd $3d_{5/2}$ and Pd $3d_{3/2}$ peaks at binding energies of 335.0 and 340.2 eV, respectively. The Pd $3d_{5/2}$ electron binding energy for NWs or NPs is 335.7 or 336.4 eV, respectively. A comparison of these values with the Pd $3d_{5/2}$ electron binding energies for Pd^0, PdO, and PdO_2 nanophases, 335.1 vs 335.4, 336.8 vs 337.2, and 337.8 vs 339.3 eV, respectively [24, 25], leads to the conclusion that the nanowires and nanoparticles are palladium metal externally coated with an oxide film.

Catalytic Behavior of Nanowires and Nanoparticles

Figure 2a shows the dependence of CO conversion upon the pulsed injection number for the case of successive elevation of the reactor temperature. It is seen that the nanowires exhibit catalytic activity only when heated to 523 K. At a fixed temperature in the range of 548–623 K, the CO conversion increases from pulse to pulse, reaching a steady-state value of $67 \pm 2\%$ after 7–15 injections. It is interesting that after purging the reactor with helium for the subsequent step to a higher temperature, the initial CO conversion and, hence, activity of the sample decreased, and increased to higher steady-state values only after several successive injections of the reaction mixture. It was not until

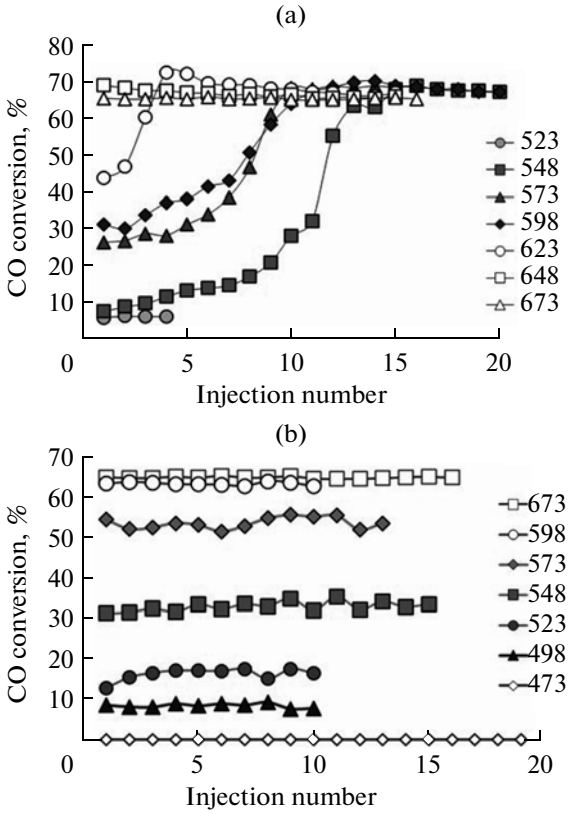

Fig. 2. Dependence of CO conversion upon the injection pulse number for nanowires with (a) increasing or (b) decreasing temperature (T, K).

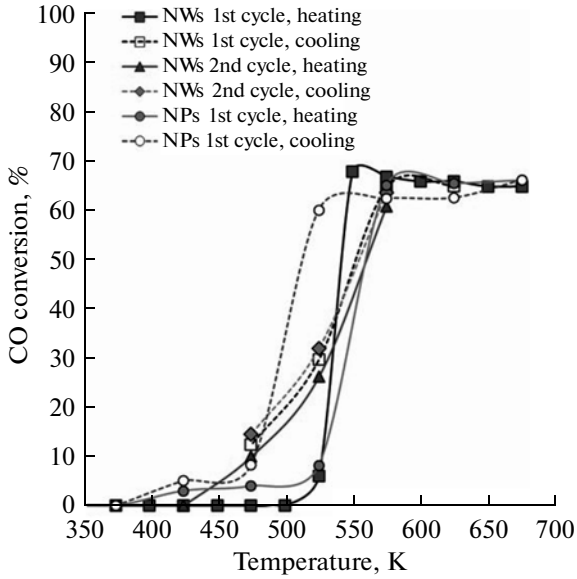

Fig. 3. Temperature dependence of steady-state CO conversion on nanowires and nanoparticles with a stepwise increase or decrease in temperature.

heating the nanowires over 623 K that the CO conversion reached 67% immediately after the 1st pulse and remained independent of temperature anymore. Nanowire testing at temperatures successively lowered from 723 to 598 K showed that catalyst "conditioning" is eliminated and the steady-state CO conversion value of 67% is achieved now after the first injection of the reactants (Fig. 2b). A further decrease in temperature from 598 to 498 K leads to a gradual reduction of the steady-state CO conversion from 67 to 9%. In this case, a steady-state value of the CO conversion is also achieved with the first injection.

Figure 3 shows the temperature dependence of steady-state values of CO conversion. It can be seen that the temperature dependence of CO conversion becomes less sharp in the second cycle of NW testing; the conversion values are at close levels in the both heating and cooling modes. Despite the fact that the CO oxidation on NWs and NPs occurs in close temperature ranges, their catalytic behaviors are not completely identical. The main difference is due to the reversible "conditioning" of nanowires, which was not observed in the comparative experiments with nanoparticles (Figs. 4a, 4b). The maximal CO conversions on the NWs and NPs differ insignificantly, making $67 \pm 2\%$ (reached at 548 K) and $63 \pm 2\%$ (reached at 573 K) as shown in Fig. 3. But in the case of cooling, the high CO conversion on NPs, $63 \pm 2\%$, is retained to 523 K, whereas that for NWs drops to 17% already at this temperature (Figs. 4b, 2b).

A full understanding of the reasons behind the differences in catalytic behavior between the nanowires and nanoparticles, especially, in the ability of nanowires for "conditioning", requires more detailed investigation. But there are a few possible reasons that can be discussed at the moment. First of all, the conditioning of NWs under isothermal conditions can be associated with their disintegration into separate fragments as demonstrated in Figs. 1a and 1c, but it should be noted that the cause of collapse of the nanowires is Rayleigh instability; so the total surface area of the metal is not to vary during disintegration [26]. Furthermore, the disintegration of nanowires cannot explain the changes in their activity in the temperature range of 548–623 K in view of reversibility of this effect. The likely cause of the different behaviors of the NWs and NPs is differences in the Pd electronic state, which changes during the course of the reaction. According to the XPS data, palladium occurs in both the metal and oxidized states on the NW and NP surface; it is also known [24] that the catalyst activity is determined by the Pd(0)/Pd($+n$) ratio. This ratio may vary, as well as the ability of Pd and PdO_x to be oxidized by O_2 and reduced by CO, respectively, on the NW and NP surface. It also cannot be excluded that the set of edges and defects on the NW and NP surfaces, which determines the adsorption and, hence, catalytic properties, may differ and vary under the influence of both temperature and adsorbed reactant and product molecules during the catalysis. Such phe-

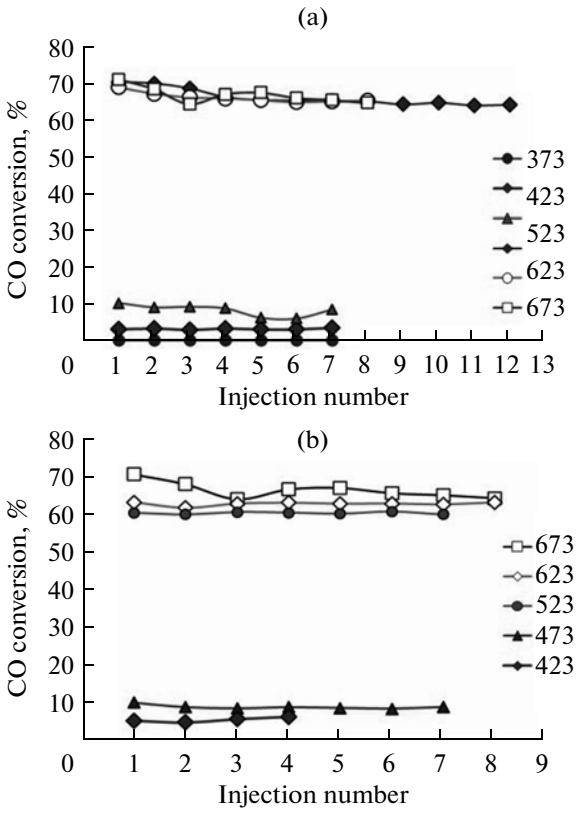

Fig. 4. Dependence of CO conversion upon the injection pulse number for nanoparticles with (a) increasing or (b) decreasing temperature (T, K).

nomena are being actively discussed in the contemporary scientific literature [2, 27–30].

CONCLUSIONS

The main achievement is the proof that the amount of a palladium-nanowire web obtained using the exotic low-temperature method is sufficient for the direct determination of its catalytic activity in a standard catalytic unit. Furthermore, the procedure of nanoweb deposition on the filter surface has appeared beneficial both in terms of reliable nanoweb fixation and high efficiency of diffusion transport of the reactants from the feed stream to the catalyst surface. Unfortunately, the catalytic activity observed is presumably due to electrically unconnected nanowire fragments, rather than the initial nanowires. Thus, even the use of palladium, a quite refractory metal, does not make it possible to save the nanoweb of nanowires as a whole entity at temperatures above 623 K.

At the same time, the results of this work allow us to formulate the following lines of further research in application of nanowebs in nanocatalysis.

(1) Use of nanowires in catalytic processes occurring at lower temperatures. In particular, the temperature of CO oxidation on nanowires can be lowered by increasing the oxygen content in the reaction mixture, as it has been done in the case of PtFe–FeO_x nanowires supported on the TiO_2 surface [8]. In addition, nanowires can hold promise for use in liquid-phase catalysis, which is usually conducted at temperatures not exceeding 400 K.

(2) Making nanowires from more refractory metals (primarily, Nb) exhibiting good activity in nanocatalysis.

(3) Development of methods for the synthesis of core–shell nanowires, the stability of which is determined by the core material. Tungsten can be used as a core material, and catalytic properties will be determined by the nature of the shell, which can be made of different, catalytically active and not necessarily refractory metal, e.g., silver or gold.

ACKNOWLEDGMENTS

This work was supported by the Russian Science Foundation, project no. 14-13-00574. The equipment used to determine catalytic activity was purchased under the Moscow State University Development Program.

REFERENCES

1. Freund, H.-J., Meijer, G., Scheffler, M., Schlogl, R., and Wolf, M., *Angew. Chem. Int. Ed.*, 2011, vol. 50, no. 43, p. 10064.
2. Royer, S. and Duprez, D., *ChemCatChem*, 2011, vol. 3, p. 24.
3. Ellert, O.G., Tsodikov, M.V., Nikolaev, S.A., and Novotortsev, V.M., *Usp. Khim.*, 2014, vol. 83, no. 8, p. 718.
4. Nikolaev, S.A., Golubina, E.V., Kustov, L.M., Tarasov, A.L., and Tkachenko, O.P., *Kinet. Catal.*, 2014, vol. 55, no. 3, p. 311.
5. McClure, S.M. and Goodman, D.W., *Chem. Phys. Lett.*, 2009, vol. 469, nos. 1–3, p. 1.
6. Cuenya, B.R., *Thin Solid Films,* 2010, vol. 518, p. 3127.
7. Uzio, D. and Berhault, G., *Catal. Rev.: Sci. Eng.*, 2010, vol. 52, no. 1, p. 106.
8. Zhu, H., Wu, Z., Su, D., Veith, G.M., Lu, H., Zhang, P., Chai, S.-H., and Dai, S., *J. Am. Chem. Soc.*, 2015, vol. 137, no. 32, p. 10156.
9. Gordon, E.B., Karabulin, A.V., Matyushenko, V.I., Sizov, V.D., and Khodos, I.I., *Phys. Chem. Chem. Phys.*, 2014, vol. 16, no. 46, p. 25229.
10. Lebedev, V., Moroshkin, P., Grobety, B., Gordon, E., and Weis, A., *J. Low Temp. Phys.*, 2011, vol. 165, no. 3, p. 166.
11. Gordon, E.B., Karabulin, A.V., Morozov, A.A., Matyushenko, V.I., Sizov, V.D., and Khodos, I.I., *J. Phys. Chem. Lett.*, 2014, vol. 5, no. 7, p. 1072.
12. Gordon, E.B., Karabulin, A.V., Matyushenko, V.I., Rostovshchikova, T.N., Nikolaev, S.A., Lokteva, E.S., and Golubina, E.V., *Gold Bull.*, 2015. doi: 10.1007/s13404-015-0168-y

13. Gordon, E.B., Karabulin, A.V., Matyushenko, V.I., and Khodos, I.I., *Journal of Physical Chemistry*, 2015, vol. 119, no. 11, p. 2490.
14. Gordon, E.B. and Okuda, Y., *Journal of Low Temperature Physics*, 2009, vol. 35, no. 3, p. 209.
15. Loubat, A., Lacroix, L.-M., Robert, A., Imperor-Clerc, M., Poteau, R., Maron, L., Arenal, R., Pansu, B., and Viau, G., *J. Phys. Chem.*, 2015, vol. 119, no. 8, p. 4422.
16. Guo, S., Li, D., Zhu, H., Zhang, S., Markovic, N.M., Stamenkovic, V.R., and Sun, S., *Angew. Chem. Int. Ed.*, 2013, vol. 52, no. 12, p. 3465.
17. Rostovshchikova, T.N., Smirnov, V.V., Gurevich, S.A., Kozhevin, V.M., Yavsin, D.A., Nevskay, S.M., Nikolaev, S.A., and Lokteva, E.S., *Catal. Today*, 2005, vol. 105, no. 3/4, p. 344.
18. Lokteva, E.S., Peristyy, A.A., Kavalerskaya, N.E., Golubina, E.V., Yashina, L.V., Rostovshchikova, T.N., Gurevich, S.A., Kozhevin, V.M., Yavsin, D.A., and Lunin, V.V., *Pure Appl. Chem.*, 2012, vol. 84, no. 3, p. 495.
19. Rostovshchikova, T.N., Shilina, M.I., Golubina, E.V., Lokteva, E.S., Krotova, I.N., Nikolaev, S.A., Maslakov, K.I., and Yavsin, D.A., *Izv. Akad. Nauk, Ser. Khim.*, 2015, no. 4, p. 812.
20. Lokteva, E.S., Rostovshchikova, T.N., Kachevskii, S.A., Golubina, E.V., Smirnov, V.V., Stakheev, A.Yu., Telegina, N.S., Gurevich, S.A., Kozhevin, V.M., and Yavsin, D.A., *Kinet. Catal.*, 2008, vol. 49, no. 5, p. 748.
21. Nikolaev, S., Pichugina, D., and Mukhamedzyanova, D.F., *Gold Bull.*, 2012, vol. 45, no. 4, p. 221.
22. Nikolaev, S.A., Chistyakov, A.V., Chudakova, M.V., Kriventsov, V.V., Yakimchuk, E.P., and Tsodikov, M.V., *J. Catal.*, 2013, vol. 297, p. 296.
23. Nikolaev, S.A., Golubina, E.V., Krotova, I.N., Shilina, M.I., Chistyakov, A.V., and Kriventsov, V.V., *Appl. Catal., B*, 2015, vol. 168/169, p. 303.
24. Ivanova, A.S., Slavinskaya, E.M., Gulyaev, R.V., Zaikovskii, V.I., Stonkus, O.A., Danilova, I.G., Plyasova, L.M., Polukhina, I.A., and Boronin, A.I., *Appl. Catal., B*, 2010, vol. 97, p. 57.
25. Mirkelamoglu, B. and Karakas, G., *Appl. Catal., A*, 2006, vol. 299, p. 84.
26. Volk, A., Knez, D., Thaler, P., Hauser, A.W., Grogger, W., Hofer, F., and Ernst, W.E., *Phys. Chem. Chem. Phys.*, 2015, vol. 17, p. 24570.
27. Small, M.W., Sanchez, S.I., Marincovic, N.S., Frenkel, A.I., and Nuzzo, R.G., *ACS Nano*, 2012, vol. 6, no. 6, p. 5583.
28. Alia, S.M., Duong, K., Liu, T., Jensen, K., and Yan, Y., *ChemSusChem*, 2012, vol. 5, no. 8, p. 1619.
29. Zarechnaya, E.Yu., Skorodumova, N.V., Simak, S.I., Johansson, B., and Isaev, E.I., *Comput. Mater. Sci.*, 2008, vol. 43, no. 3, p. 522.
30. Hannevold, L., Nilsen, O., Kjekshus, A., and Fjellvag, H., *Appl. Catal., A,* 2005, vol. 284, no. 1/2, p. 185.

Translated by S. Zatonsky

SPELL: 1. OK